Article:
Okoro-Shekwaga, CK, Ross, AB and Camargo-Valero, MA orcid.org/0000-0003-2962-1698 (2021) Enhanced in-situ biomethanation of food waste by sequential inoculum acclimation: Energy efficiency and carbon savings analysis. Waste Management, 130. pp. 12-22. ISSN 0956-053X

https://doi.org/10.1016/j.wasman.2021.04.053

Okoro-Shekwaga C K, Ross A B, Camargo-Valero M A (2021). Enhanced in-situ biomethanation of food waste by sequential inoculum acclimation: energy efficiency and carbon savings analysis. *Waste Management*,130, 12-22. doi:10.1016/j.wasman.2021.04.053

Enhanced *in-situ* biomethanation of food waste by sequential inoculum acclimation: energy efficiency and carbon savings analysis.

Cynthia Kusin OKORO-SHEKWAGA[a,c], Andrew Barry ROSS[b] and Miller Alonso CAMARGO-VALERO[a,d*]

[a] BioResource Systems Research Group, School of Civil Engineering, University of Leeds, Leeds LS2 9JT, United Kingdom
[b] School of Chemical and Process Engineering, University of Leeds, Leeds LS2 9JT, United Kingdom.
[c] Department of Agricultural and Bioresources Engineering, Federal University of Technology, Minna, P.M.B. 65, Niger State Nigeria
[d] Departamento de Ingeniería Química, Universidad Nacional de Colombia, Campus La Nubia, Manizales, Colombia
*Corresponding author. Tel.: +44 (0)113-34-31580
E-mail address: M.A.Camargo-Valero@leeds.ac.uk (Miller Alonso Camargo-Valero)

Abstract

The increasing rate of food waste (FW) generation globally, makes it an attractive resource for renewable energy through anaerobic digestion (AD). The biogas recovered from AD can be upgraded by the methanation of internally produced carbon dioxide, CO_2 with externally sourced hydrogen gas, H_2 (biomethanation). In this work, H_2 was added to AD reactors processing FW in three successive phases, with digestate from preceding phases recircled in succession with the addition of fresh inoculum to enhance acclimation. The concentration of H_2 was increased for succeeding phases: 5%, 10% and 15% of the reactor headspace in Phase 1 (EH1), Phase 2 (EH2) and Phase 3 (EH3), respectively. The H_2 utilisation rate and biomethane yields increased as acclimation progressed from EH1 through EH3. Biomethane yield from the controls: EH1_Control, EH2_Control and EH3_Control were 417.6, 435.4 and 453.3 NmL-CH_4/gVS_{added} accounting for 64.8, 73.9 and 77.8% of the biogas respectively. And the biomethane yield from the test reactors EH1_Test, EH2_Test and EH3_Test were 468.3, 483.6, and 499.0 NmL-

CH_4/gVS_{added}, accounting for 77.2, 78.1 and 81.0% of the biogas respectively. A progressive *in-situ* biomethanation could lead to biomethane production that meets higher fuel standards for gas-to-grid (GtG) injections and vehicle fuel – i.e. >95% CH_4. This would increase the energy yield and carbon savings compared to conventional biogas upgrade methods. For example, biogas upgrade for GtG by *in-situ* biomethanation could yield 7.3 MWh/t_{FW} energy and 1,343 kg-CO_2e carbon savings, which is better than physicochemical upgrade options (i.e., 4.6–4.8 MWh/t_{FW} energy yield and 846–883 kg-CO_2e carbon savings).

Keywords

Biomethanation; Hydrogen; Food waste; Biomethane; Energy balance; Carbon saving.

1. Introduction

Evolving population and socio-economic growth are influencing increasing levels of food waste (FW) generation around the world (Uçkun Kiran et al., 2014). Currently, 1.4 billion tonnes (Bt) of food is wasted every year worldwide and it is estimated by the UN Food and Agriculture Organization (FAO) to exceed 2.2 Bt by 2025 (Gu et al., 2020). Based on data generated between 2011 and 2015, the Waste Resource and Action Programme (WRAP) in the United Kingdom (UK), estimated the annual FW arising in the UK to be 10 million tonnes (Mt), equivalent to a quarter of the 41 Mt of food purchased annually in the UK (WRAP, 2017). To avoid the environmental impacts related to FW decomposition in landfills, including greenhouse gas (GHG) emissions and associated global climate changes, contamination of groundwater sources by leachate, heat losses and odour emissions (Girotto et al., 2015; Mirmohamadsadeghi et al., 2019), anaerobic digestion (AD) is widely accepted among other renewable technologies to treat and recover energy from FW (Gu et al., 2020).

Energy can be recovered through the AD process in the form of methane-rich biogas, which is typically composed of 50 – 70% methane (CH_4) and 30 – 50% carbon dioxide (CO_2) (Angelidaki et al., 2018). AD of FW is seen to play a key role in

63 reducing direct carbon emissions from FW to the environment. It was reported that
64 the amount of methane captured from the AD of 1 tonne of FW would potentially
65 save 0.5-tonne CO_2 equivalent (tCO_2e) from its disposal in landfills (Defra, 2011;
66 Evangelisti et al., 2014). In this regard, it was postulated that the production of CH_4
67 from the organic fraction of municipal solid waste amounts to about 79% GHG
68 savings when compared to the fossil fuel it displaces (Rajendran et al., 2019). To
69 further reduce the carbon (CO_2) arising from AD and also improve the calorific value
70 of biogas to higher fuel standards and thus, its end-use, adaptable biological
71 hydrogen (H_2) methanation (biomethanation) is gaining increasing interest (Wahid et
72 al., 2019).
73 Biomethanation involves enhancing the H_2/CO_2 route for CH_4 production during AD
74 (hydrogenotrophic methanogenesis) by the addition of externally sourced H_2 (Wahid
75 et al., 2019). Biomethane content in the range of 65 – 100% has been reported by
76 previous biomethanation studies using relatively low organic substrates such as
77 cattle slurry and microalgae (Tian et al., 2018), potato-starch wastewater (Bassani
78 et al., 2016) and maize leaf (Mulat et al., 2017) among others. The use of FW as a
79 substrate is highly under-developed and limited to few recent studies (Okoro-
80 Shekwaga et al., 2019; Tao et al., 2020, 2019). FW can provide a suitable pH buffer
81 during *in-situ* biomethanation due to high levels of volatile fatty acids (VFA) produced
82 from its fermentation (Okoro-Shekwaga et al., 2019). Moreover, the growing rate of
83 FW around the world makes it a competitive resource for sustainable renewable
84 energy generation via biomethanation, especially as renewable energy technologies
85 face major drawbacks due to limited resources against a competing more abundant
86 fossil sources (Rajendran et al., 2019).
87 Exogenous H_2 loading to an AD system could increase the H_2 partial pressures up
88 to levels that stall the decomposition of VFA intermediates, leading to accumulation
89 and possible process failure (Mulat et al., 2017). The decomposition of common VFA
90 intermediates during AD, including butyrate and propionate, are endergonic as
91 shown in Equation 1 and Equation 2, which means the forward reactions would not
92 be spontaneous and could very easily stop at high concentrations of dissolved H_2

and acetate (Mulat et al., 2017). However, Fukuzaki et al. (1990) reported a reversal of inhibitions to propionate decomposition when H_2 removal was enhanced.

$$CH_3(CH_2)_2COO^- + 2H_2O \leftrightarrow 2CH_3COO^- + 2H_2 + H^+ \quad \Delta G^0 = +48.3\ kj/mol \quad \textit{Eq. 1}$$

$$CH_3CH_2COO^- + 3H_2O \leftrightarrow CH_3COO^- + H^+ + HCO_3{}^- + 3H_2 \quad \Delta G^0 = +76.1\ kj/mol \quad \textit{Eq. 2}$$

Previous studies suggest that exposing AD consortia to increasing levels of inhibitory substances including ammonia (NH_3) (Gao et al., 2015), long-chain fatty acids (LCFA), toxic metals and phenolic compounds, allow them to adapt to and overcome the inhibitory effects; a process known as acclimation (Chen et al., 2008). This is generally brought about by a shift in the microbial population or internal changes that occur in the predominant species within microbial consortia (Chen et al., 2008). As in the present investigation, acclimation can be employed to allow AD reactors to gradually adjust to high H_2 loads during *in-situ* biomethantion and thus, avoid VFA accumulation and associated process instability. For instance, Agneessens et al. (2017) found that methanogen adaptation by pulse H_2 addition improved H_2 gas-liquid mass transfer rate, thus, lowering H_2 partial pressure by enhanced biomethanation.

The present work investigated the upgrade of biogas from FW by *in-situ* biomethanation, with a focus on how acclimating the system to a stepwise increase in H_2 load affects the H_2 utilisation rate and reversal of VFA accumulation. The present study also includes a comparative energy return on investment (EROI) and carbon savings for biogas upgrade between *in-situ* biomethanation and typical physicochemical technologies. Therefore, this manuscript demonstrates the novelty of FW valorisation by *in-situ* biomethanation for clean bioenergy production and how stepwise acclimation to increasing concentrations of H_2 could improve the efficiency of H_2/CO_2 conversion to biomethane during *in-situ* biomethanation. It demonstrates how FW, which is currently a global environmental hazard, can be used to substantially increase the share of renewable energy in the global energy mix.

2. Methodology

Three sets of experiments were assayed in sequential phases (EH1, EH2 and EH3) to analyse the combined impact of system acclimation to H_2 and increasing H_2 concentration on *in-situ* biomethanation using FW as a substrate (see Section 2.1). For each phase a blank (inoculum only), control (inoculum + FW) and test (inoculum + FW + H_2) was assayed. Acclimation was achieved by mixing fresh inoculum with digestate from a previous phase, which had gone through *in-situ* biomethanation (test) at lower H_2 dosing (see Section 2.2).

2.1 Food waste source and processing

Waste samples were collected over 5 days from the kitchen and dining areas (leftovers in plates) of the University of Leeds' student refectory in separately monitored bins. The collected waste samples were manually sorted daily after each collection to separate the FW from the unwanted materials such as plastics, metals and papers and the FW fraction was stored daily at 4 ˚C until the last day of sampling (Day 5). After the collection period, segregated FW samples were first minced using a manual mincing machine and then blended with a Nutribullet food processor to obtain a paste. The blended FW was then sieved through a 1 mm sieve to achieve a homogenised sample with a 1 mm particle size range. A portion of the homogenised FW was stored in the refrigerator at 4 °C for preliminary

characterisation (

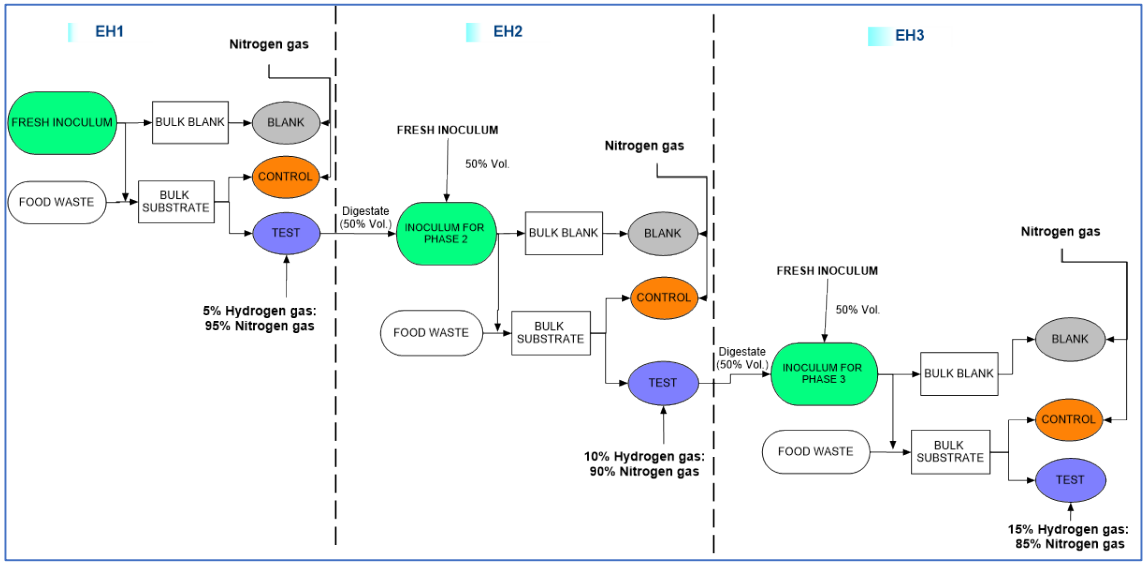

Figure 1. Experimental design for enhanced biomethanation from food waste via sequential inoculum acclimation by H_2 addition

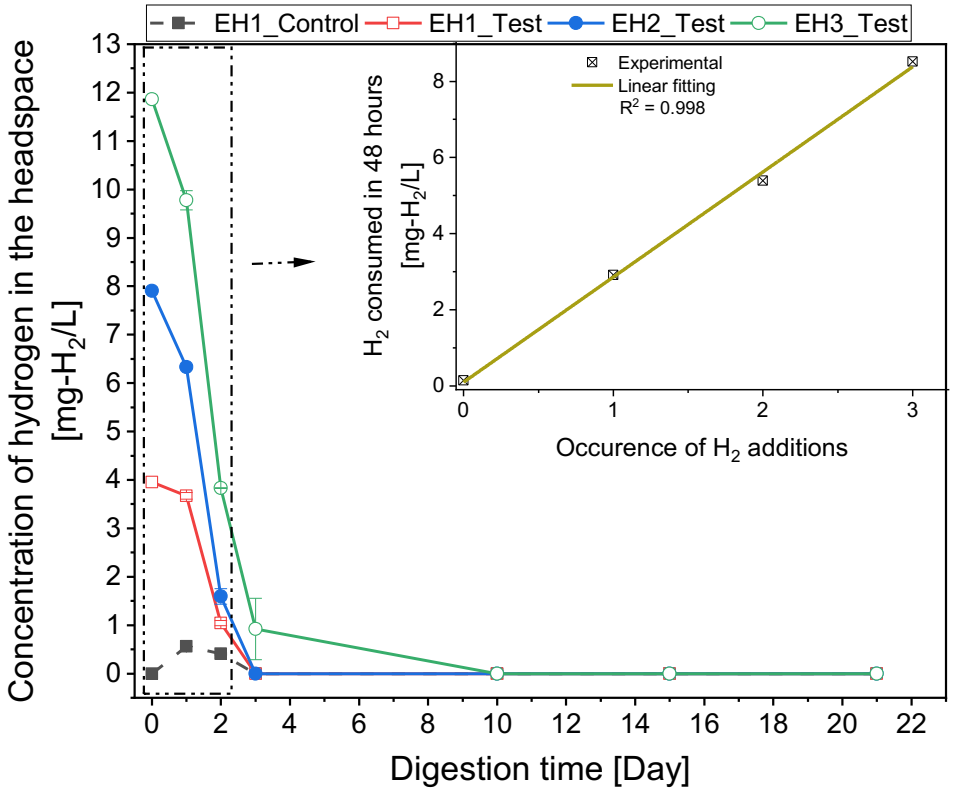

Figure 2. Changes in headspace H_2 concentration as an indication of H_2 gas-liquid transfer (H_2 was not detected in EH2_Control and EH3_Control).

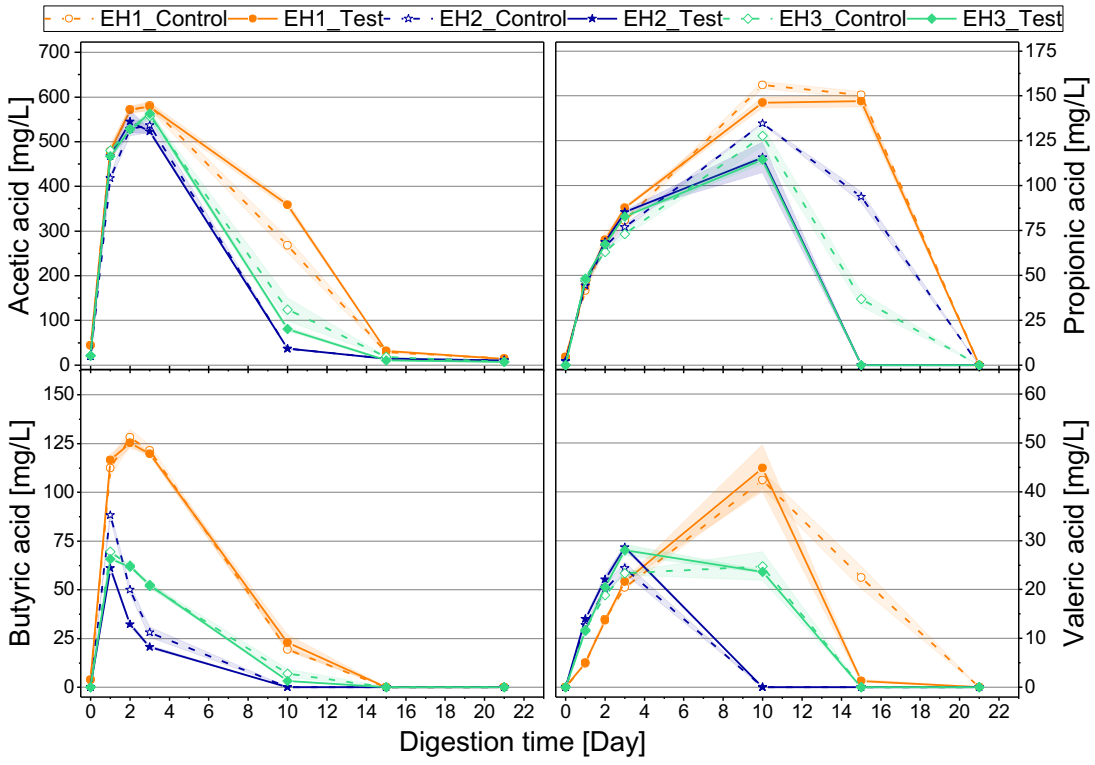

148

149 *Figure 3. Effects of hydrogen acclimation on VFA composition: test values*
150 *presented in solid lines and control in dash lines. The shaded area*
151 *around the lines represents the standard deviation from the mean.*

152

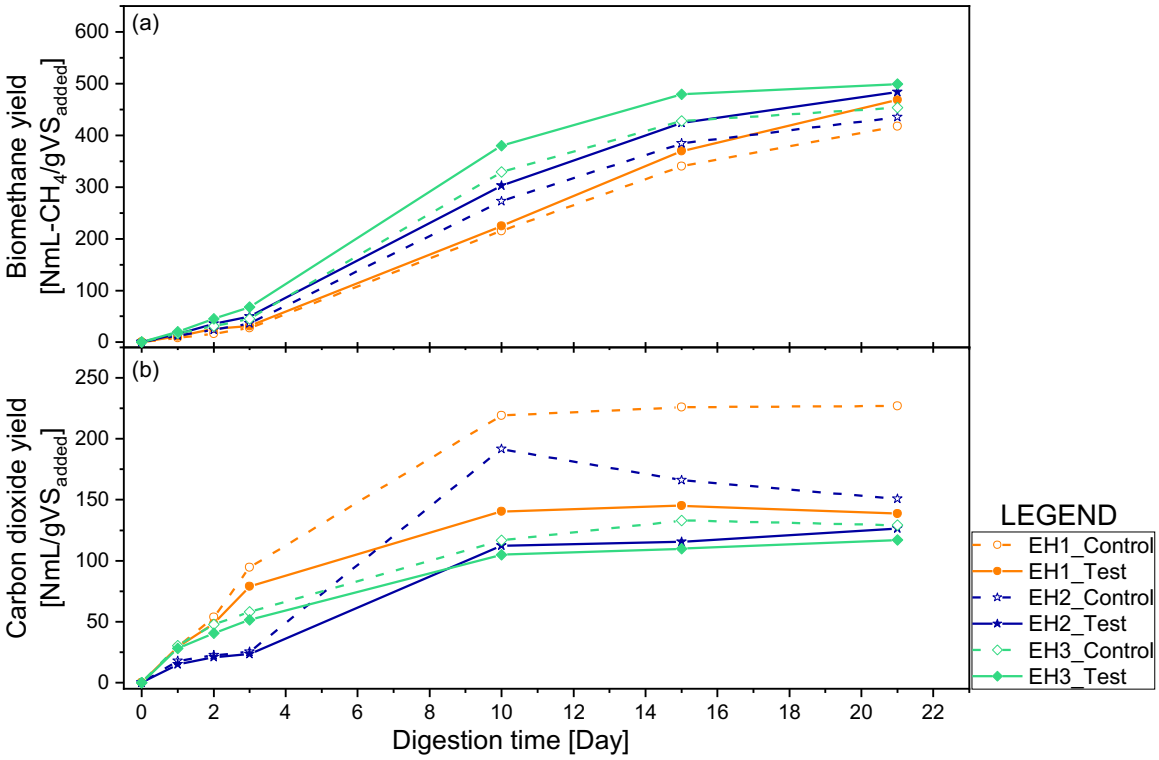

153

154 *Figure 4. Biomethane (a) and Carbon dioxide (b) production curves from all*
155 *hydrogen-based acclimation experiments: dash lines represent*
156 *control yields and the solid lines represent test yields.*

Table 1), conducted within 14 days to reduce any possible error due to deterioration. The rest of the homogenized FW was transferred into refrigerator bags, sealed and stored at -20 °C until needed for the respective experiments. For *in-situ* biomethanation experiments, frozen FW samples were thawed at 4 °C for 1 – 2 days before the setup (Treu et al., 2018), so, no heat was applied to defrost the samples.

2.2 Inoculum

Sewage sludge digestate was obtained from a mesophilic anaerobic digester treating sewage sludge at Yorkshire Water's Esholt Waste Water Treatment Works, Bradford, United Kingdom (UK). The fresh inoculum was prepared by first removing grits and large materials from the sewage sludge digestate by filtering it through a 1-mm sieve and storing it at 37 °C for two weeks to remove residual biogas from the digestate. This was followed by an adaptation to FW for 30 days, achieved by adding 0.2 g-FW/(L·day). The fresh inoculum was used to seed the blank, control and test reactors in phase 1 (EH1). The fresh inoculum (50% vol.) was mixed with the digestate arising from the test reactor of EH1 (50% vol.) and used as seed for the blank, control and test reactors in phase 2 (EH2). In phase 3 (EH3), fresh inoculum (50% vol.) was mixed with the digestate arising from the test reactor of EH2 (50% vol.) and used to seed the blank, control and test reactors. The assays were not corrected for pH to avoid any interference with the added H_2. Hence, the starting pH in all experiments was largely dependent on the pH of the seed used in each

177 experimental setup; initial reactor characteristics for each phase are reported in

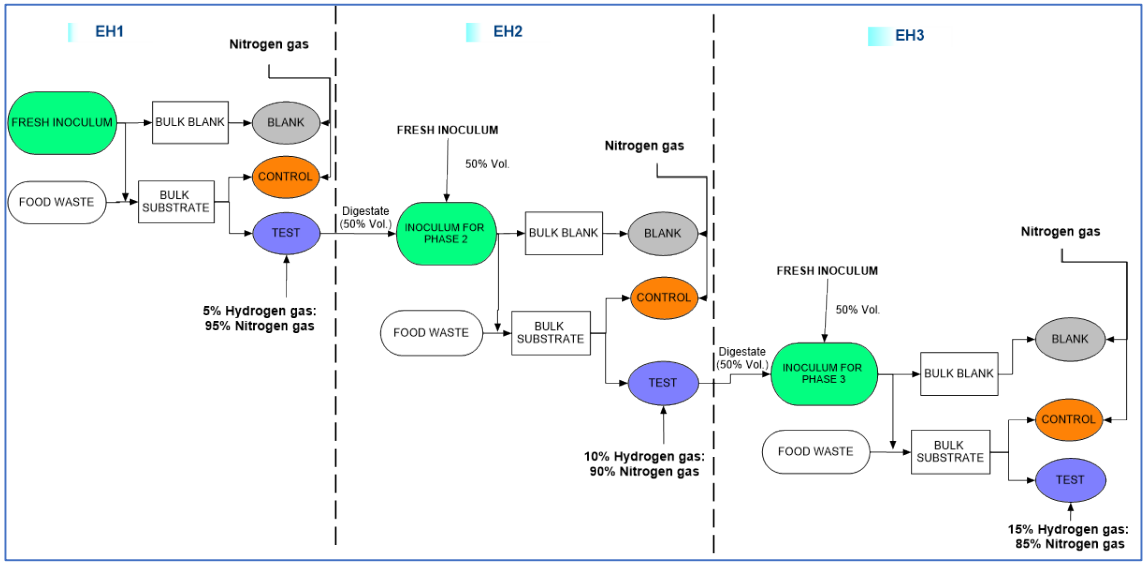

178

179 *Figure 1. Experimental design for enhanced biomethanation from food waste*
180 *via sequential inoculum acclimation by H_2 addition*

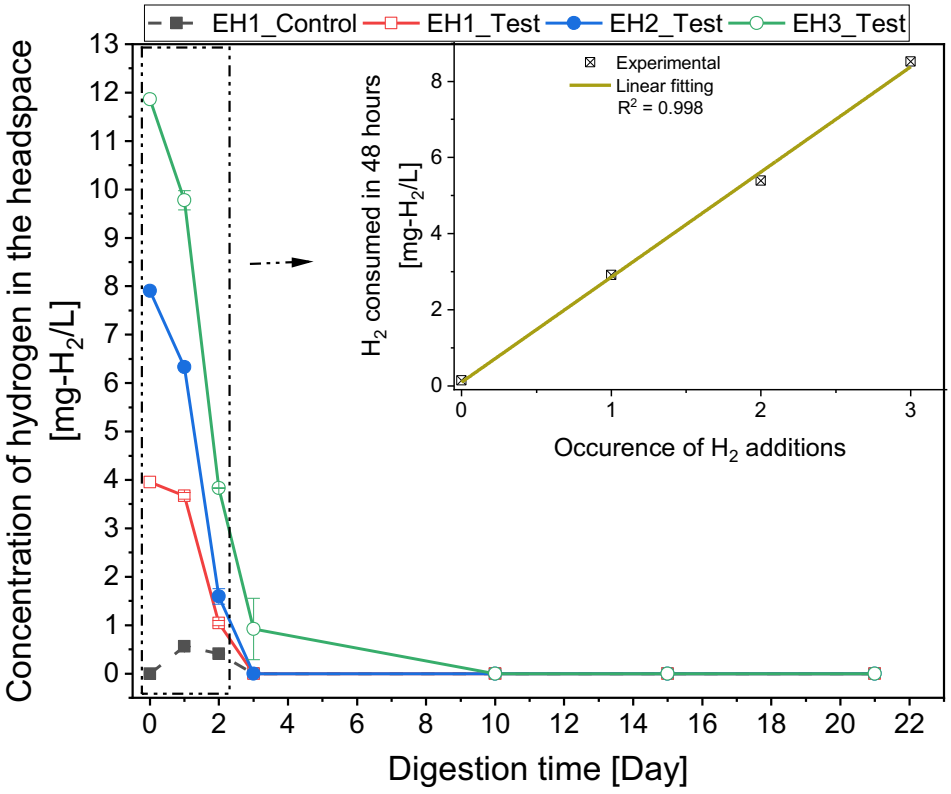

Figure 2. Changes in headspace H_2 concentration as an indication of H_2 gas-liquid transfer (H_2 was not detected in EH2_Control and EH3_Control).

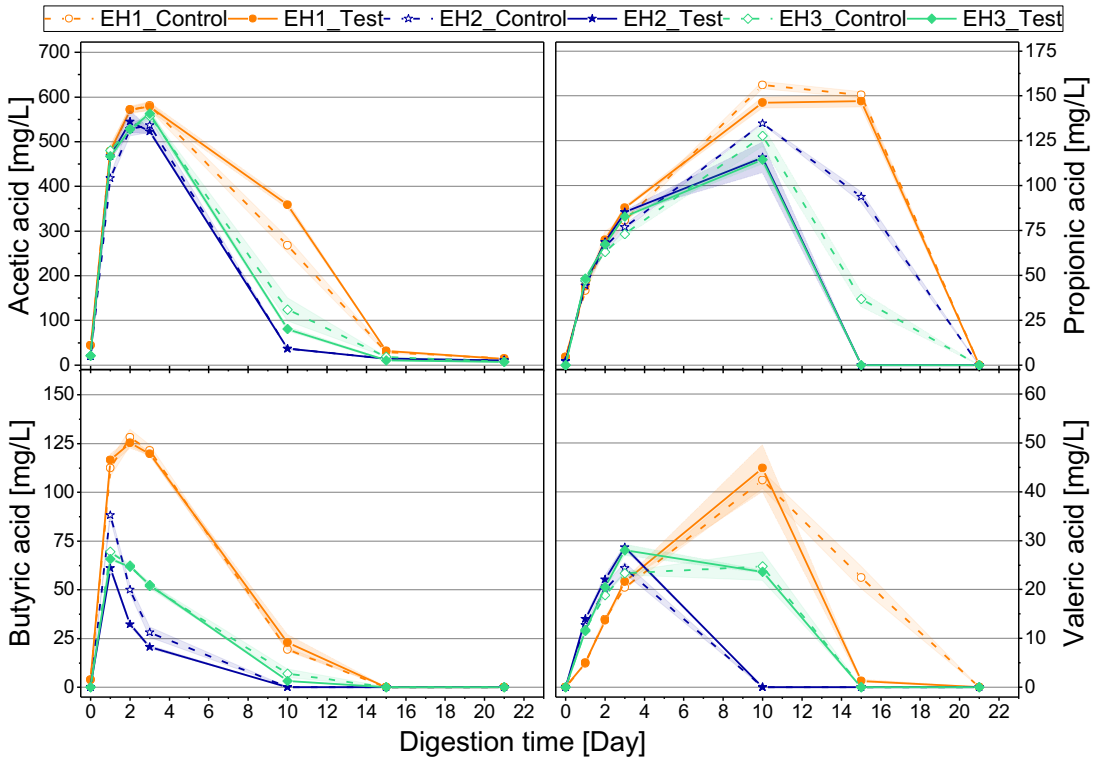

186

187 *Figure 3. Effects of hydrogen acclimation on VFA composition: test values*
188 *presented in solid lines and control in dash lines. The shaded area*
189 *around the lines represents the standard deviation from the mean.*

190

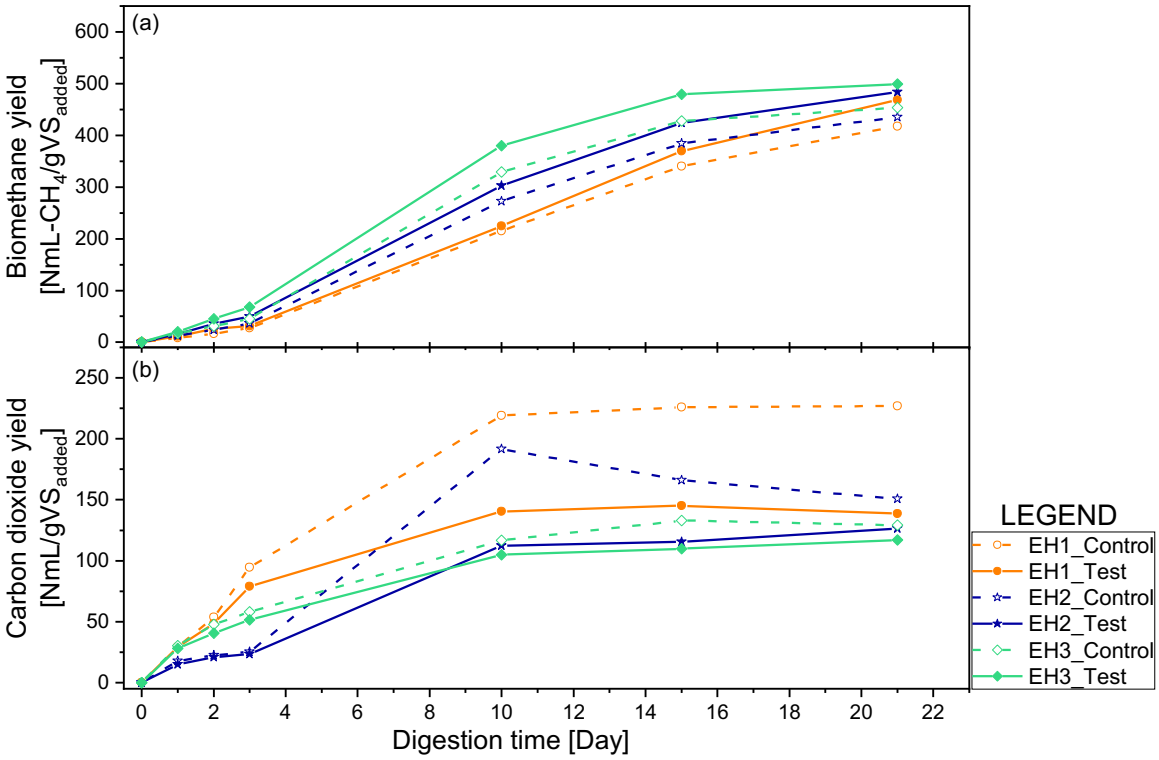

Figure 4. Biomethane (a) and Carbon dioxide (b) production curves from all hydrogen-based acclimation experiments: dash lines represent control yields and the solid lines represent test yields.

Table 1. A description of the analytical methods adopted for characterising the liquid samples is reported in Section 2.3.2.

2.3 Experimental set-up

Batch experiments were set up at mesophilic temperature (37 °C) using 160 mL (absolute volume) Wheaton bottles as anaerobic reactors at 75 mL working volume, and inoculum to substrate ratio (ISR) of 3:1 (Okoro-Shekwaga et al., 2019). The reactors were held in a water bath to maintain the temperature at 37 °C and the experiments were terminated by day 21 having attained at least 3 consecutive days of daily methane production <1% of the cumulative methane volume (Holliger et al., 2016).

H_2 addition follows a previously developed method by Okoro-Shekwaga et al. (2019), which included H_2 leak testing. H_2 was added to the test reactors of EH1, EH2 and EH3; hereafter referred to as EH1_Test, EH2_Test and EH3_Test, using a gas mixture of H_2 and nitrogen (N_2) at 5:95, 10:90 and 15:85 (% v/v) respectively (**Error! Reference source not found.**), purging for 1 min at a gas flow rate of 1000 mL/min. The control reactors of EH1, EH2 and EH3; hereafter referred to as EH1_Control, EH2_Control and EH3_Control respectively, and the blank reactors were purged with N_2 to achieve an anaerobic environment at the same flow rate and purge time as the test reactors. All reactors were prepared in triplicate for each analytical point (eight per assay) as sacrificial samples. The biogas yields (CH_4 and CO_2) from the control and test reactors of each experiment was corrected by subtracting the corresponding biogas from the blank to account for the contribution of the same.

2.3.1 Gaseous sampling and analysis

The headspace gas composition was measured by a gas chromatograph, GC (Agilent Technology, 7890A) equipped with a thermal conductivity detector (TCD) and a Carboxen 1010 PLOT column – i.e., length 30 m, diameter 0.53 mm and film thickness 30 µm. The GC-TCD was operated at 200 °C inlet temperature and 230 °C detector temperature with Argon as carrier gas (3 mL/min). Gas samples were collected from the headspace of the reactors to analyse their composition using a 500 µL glass syringe. Two full syringes were drawn and expelled through a bottle of distilled water to flush the syringe and ensure the needle was not blocked with septa cores. With the needle in the reactor, the syringe was pumped about seven times to

mix the headspace gas sample and 200 µL of headspace gas was drawn and manually injected into the GC inlet column. The GC method was calibrated with three standard gas mixtures; 50%CH_4:3%H_2:47%N_2, 20%O_2:80%N_2, and 10%CO_2:90%N_2 at predetermined intervals. After sample collection for headspace gas composition analysis, the remaining gas volume in each of the reactors was measured using a water displacement method. The water displacement setup was calibrated with 10 mL of lab air before each analysis to ensure the system pressure was maintained. The total volume of biogas produced was equal to the volume of gas collected for GC analysis plus the volume measured from water displacement.

2.3.2 Liquid analysis

The pH of the liquid samples was measured directly using a HACH pH meter (HQ 40d). TS and VS were measured by the gravimetric method as described in methods 2540B and 2540E by APHA (2005; 2006), respectively. COD was analysed by the titrimetric method 5220C (APHA, 2005; 2006). VFA concentrations were measured by a GC (Agilent Technologies, 7890A) coupled with a flame ionization detector (GC-FID) and an auto-sampler; a DB-FFAP column (length 30m, diameter 0.32mm and film thickness 0.5 µm); and Helium as a carrier gas. The GC-FID operating conditions were 150 °C inlet temperature and 200 °C detector temperature. Liquid samples were adjusted to pH 2.0 using phosphoric acid and allowed to rest for 30 mins and then centrifuged at 14,000 RPM (16,000 x *g*) for 5 min, using a Technico Maxi Microcentrifuge. Afterwards, the supernatant was filtered through a 0.2-µm filter and the filtrate analysed for VFA. The GC method was calibrated with SUPELCO Volatile Acid Standard Mix, which includes acetic-, propionic-, iso-butyric-, butyric-, iso-valeric-, valeric-, iso-caproic-, caproic- and heptanoic- acids.

2.3 Statistical analysis

Experimental data were subjected to descriptive statistical analysis – i.e., normality test, mean and standard deviation. All results from each group were first individually analysed for statistical significance, using a one-sample *t*-test. Where the results showed a significant difference, a further outlier test was conducted to remove outliers, before final analysis and graphical representations. Regression analysis for the amount of headspace H_2 removed within 48 hours as acclimation progressed from EH1 through EH3 was established using Origin® statistical tool. Regression

equations were also established for biomethane yield and compositions from nine data points obtained from sequential acclimation experiments using the Minitab18® statistical tool and the regression equations were used to predict the amount of H_2 required to obtain up to 100% biomethane.

3. Results and discussions

3.1 H_2 utilisation

The percentage of gaseous H_2 utilised (U_H) was calculated using Equation 3, where *t* is the monitoring time (day) and $H_{2(t-1)}$ and $H_{2(t)}$ represent the concentration of H_2 in the headspace at day (t – 1) and day *t* respectively. Headspace H_2 levels measured through time are presented in **Error! Reference source not found.**. In the first phase, EH1, H_2 was detected in the headspace of both EH1_Control and EH1_Test, but during the acclimation phases in EH2 and EH3, H_2 was not detected in EH2_Control and EH3_Control, hence, they were not included in **Error! Reference source not found.**. The non-detection of H_2 in EH2_Control and EH3_Control would suggest that U_H was improved, which disallowed the transfer of excess H_2 to the headspace. According to **Error! Reference source not found.**, H_2 was not detected after Day 3 (except for EH3_Test), considering the actual time between Day 2 and Day 3 when the headspace H_2 was completely utilised was unknown, the amount of H_2 consumed and U_H were only calculated for the first 48 hours of the AD. For EH1_Control whereby external H_2 was not added (zero H_2 in the headspace at the start), the U_H was only calculated for H_2 measured between 24 and 48 hours.

$$U_H = \left(\frac{H_{2\,(t-1)} - H_{2\,(t)}}{H_{2\,(t-1)}}\right) \times 100 \qquad \textit{Eq. 3}$$

The amount of H_2 utilised within 24 hours more than doubled as the experiments progressed from EH1_Test (0.28 mg H_2/L) to EH2_Test (0.65 mg H_2/L) and quadrupled as experiments progressed from EH2_Test to EH3_Test (2.58 mg H_2/L). This corresponds to U_H values of 7.2%, 9.3% and 20.9% for EH1_Test, EH2_Test and EH3_Test respectively. As the experiments progressed through time, higher amounts of H_2 were removed from the headspace of the acclimated reactors between 24 and 48 hours, measuring 0.14, 2.63, 4.74 and 5.94 mg H_2/L from the EH1_Control, EH1_Test, EH2_Test and EH3_Test respectively, which corresponds

to 25.0%, 71.6%, 74.8% and 60.8% U_H. In these reactors, most of the H_2 in the headspace was consumed within 48 hours and the inset graph in **Error! Reference source not found.** shows that the amount of H_2 consumed in this time increased linearly through the acclimation phases, which confirms that during the three acclimation phases the mass transfer of hydrogen across the gas-liquid interphase did not limit hydrogen availability/consumption in the liquid mix.

It is reported that the environmental and operational conditions of AD reactors affect the performance, behaviour and final fate of the microbial community (Demirel and Scherer, 2008). Therefore, the availability of H_2 at the start of the experiment in EH1_Test is believed to have allowed a higher U_H compared to EH1_Control. Agneessens et al. (2017) demonstrated that pulse injection of H_2 to mesophilic sludge over 5 consecutive days induced a shift in the methanogenic community towards an adaptation of hydrogenotrophic methanogens, which led to the increase in the H_2 uptake rate. The same is believed to be the case in the present study as demonstrated by the non-detection of H_2 in EH2_Control and EH3_Control and the linear increase in U_H presented in the inset graph in **Error! Reference source not found.**.

3.2 Impact of inoculum acclimation on VFA profiles

The profiles of VFA including acetic, propionic, butyric and valeric acids are presented in **Error! Reference source not found.**; showing butyric acid as the combination of normal butyric and iso-butyric acids and valeric acid as a combination of normal valeric and iso-valeric acids. Simultaneous H_2 production and consumption are considered to have a key influence on VFA decomposition (Appels et al., 2008) and hence, the increment in the H_2 partial pressure due to exogenous H_2 addition into AD reactors could lead to VFA inhibition/accumulation (Agneessens et al., 2017). Since higher levels of H_2 were used in each succeeding acclimation phase, VFA accumulation, especially propionate, would have been expected in EH2 and EH3. Sequel to biomethanation with 5%-H_2 in EH1_Test, the rate of VFA degradation improved by both acclimation (EH2_Control and EH3_Control) and increasing concentration of H_2 (EH2_Test and EH3_Test), as supported by an increased H_2 utilisation rate discussed earlier in Section 3.1.

By acclimation alone, VFA accumulation generally reduced through the acclimation phases, especially for the higher VFA. In the early periods after setup (Day 0 – Day 3), accumulation of the shorter chain VFA, acetate (C2) and propionate (C3) showed similar trends in all experiments (**Error! Reference source not found.**a and 3b). But longer chain VFA, butyrate (C4) and valerate (C5) were observed to progress differently with acclimation and increasing H_2 concentration (**Error! Reference source not found.**c and 3d).

After the start of the experiments, acetate accumulation increased in all phases, which eventually peaked at quite similar levels by Day 3 (Day 2 in EH2_Control and EH2_Test –**Error! Reference source not found.**a). As AD progressed, a decline in acetate was observed, which compared to EH1_Control, was seemingly slower in the first phase of H_2 addition (EH1_Test). This could have resulted from propionate decomposition, as propionate was observed to be relatively lower in EH1_Test than EH1_Control for the same period (Day 10) as shown in **Error! Reference source not found.**b. However, as acclimation progressed from EH1 through EH3, the acetate decomposition rate increased. Therefore, despite increasing H_2 loads in EH2_Test and EH3_Test, early-stage accumulation of acetate was not observed and acetate decomposition improved after the peak was reached in the acclimation phases.

Similarly, propionate accumulation rates within the first three days after the start of the experiment were about the same in all experiments. But the peak times and propionate concentrations at the peak points dropped through the acclimation phases. Among the predominant VFA produced during AD, propionate is often the least degradable; therefore, its accumulation is sustained relatively longer during the AD period (Shi et al., 2017; Wang et al., 2006). The first phase of H_2 addition (EH1_Test) showed similar propionate profiles as the control (EH1_Control), which both had high peaks at Day 10 and maintained through Day 15. A similar observation was also made by Luo & Angelidaki (2013) whereby accumulated propionate in a control AD reactor (without hydrogen addition) was maintained up to 15 days after the start of the experiment. In the present study, as acclimation progressed to EH2_Control and EH3_Control, propionate levels dropped rather quickly after reaching relative peaks by Day 10. At the peak points, propionate levels in

EH2_Control and EH3_Control were about 13% and 18% lower than the peak level of EH1_Control. Despite increasing concentrations of H_2, propionate decomposition was observed to be further enhanced in EH2_Test and EH3_Test. Propionate levels at the peak points in EH2_Test and EH3_Test were around 14% and 10% lower than the corresponding peak point values of EH2_Control and EH3_Control respectively. An increase in propionate decomposition is often suggestively linked to an enhanced H_2 or acetate uptake rate usually by enrichment of the associated microbial (Savvas et al., 2017; Yang et al., 2017). Based on the aforementioned observation on the enhanced uptake of the exogenous headspace H_2 in the present study, it can be inferred that as acclimation progressed, the consumption of the internally produced H_2 from the oxidation of other longer-chain VFA was also enhanced, which allowed faster propionate decomposition (Lee et al., 2009). Likewise, considering that in the acclimation phases, the acetate decomposition rate increased after peak points were reached, the improvement in propionate decomposition observed could also be syntrophically linked to an accelerated acetate decomposition leading to improved biogas yields (See Section 3.3).

Propionate to acetate (P/A) ratio above 1.4 is widely accepted as a more reliable index to predict possible AD failure over the actual VFA levels (Wang et al., 2012). Generally, the P/A values in all experiments remained below 1.4 except at the propionate peak points. By acclimation, the P/A reduced from 5.17 in EH1_Control to 3.69 and 3.52 in EH2_Control and EH3_Control respectively. With a stepwise increase in the concentration of H_2 added to the acclimated system, the P/A reduced from 4.65 in EH1_Test, to 3.19 and 1.42, in EH2_Test and EH3_Test respectively. The present study, therefore, shows that sequential inoculum acclimation with a stepwise increment of H_2 loading could help to eliminate propionate accumulation, which is suggested to be the main VFA to accumulate in unstable FW anaerobic digesters (Lim et al., 2017).

Some studies suggested the use of butyrate and iso-butyrate as indicators of process instability due to their relative sensitivity to different forms of sporadic imbalances (Shi et al., 2017). Among the monitored VFA intermediates, butyrate accumulation peaked earliest after the start of the experiments. Faster butyrate decomposition compared to other VFA intermediates have also been reported in

earlier studies (Gallert and Winter, 2008; Wang et al., 1999). This was the case in all three experimental phases, and much more so in the acclimation phases. In EH1, butyrate peak concentrations were achieved by Day 2 and as acclimation progressed butyrate peaked by Day 1 in EH3. Moreover, the concentration of butyrate at the peaks in EH2_Control was 31.06% lower than the peak in EH1_Control, which further decreased by 30.85% as acclimation progressed through EH3_Control. Similar to the propionate trend, the addition of H_2 to the acclimated system in EH2_Test and EH3_Test seemed to enhance butyrate degradation even further than was observed in the respective controls, EH2_Control and EH3_Control.

Valerate (C5) was the only VFA with higher early-stage accumulation as acclimation progressed among the C2 – C5 VFA assayed. Within the first 3 days of setup, the controls and tests of the acclimation phases, EH2 and EH3, yielded higher levels of valerate than the control and test of EH1. By Day 3, the valerate levels in EH2_Control and EH3_Control were about 19.45% higher than EH1_Control. The test reactors in all three experiments had higher levels of valerate than the corresponding controls and the percentage differences between the test and the control increased with acclimation: 5.6%, 17.4% and 20.4% for EH1, EH2 and EH3 respectively. However, the time taken to reach peak values was shortened from 10 days in EH1 to 3 days in EH2 and EH3. So the high early-stage accumulation of valerate in the acclimation phases was also accompanied by a rapid decomposition in EH2 and EH3, which disallowed prolonged high peak levels.

Valerate would typically degrade to acetate, propionate and H_2 (Shi et al., 2017; Yang et al., 2015); therefore, its decomposition should ideally lead to an increase in propionate and acetate. But valerate decomposition was consistent with propionate and acetate decomposition in EH2 and EH3. This means valerate could serve as a suitable short term sink for excess dissolved H_2 since its subsequent decomposition did not lead to a build-up of acetate and propionate. The potential VFA accumulation towards valerate instead of propionate and/or acetate reported in this study due to initial H_2 concentration increases in the acclimation phases should be further explored in future studies to reduce inhibitory effects associated with high H_2 load/partial pressure during FW AD.

3.3 Biogas Upgrade

The addition of H_2 and subsequent acclimation helped to upgrade the biogas from FW AD, which agrees in general with previous studies on biomethanation (Angelidaki et al., 2018). Acclimation to increasing levels of H_2 improved the biomethane yield and the biogas quality is presented in **Error! Reference source not found.**, which shows the yield from the H_2-supplemented assays (EH1_Test, EH2_Test and EH3_Test) in solid lines and the control (EH1_Control, EH2_Control and EH3_Control) in dash lines. EH2_Control and EH3_Control were observed to have improved biogas quality, especially in terms of CO_2 reduction compared to EH1_Control, which had the highest amount of CO_2 in the biogas.

Biomethane yield increased from 417.6 NmL-CH_4/gVS_{added} in EH1_Control to 435.4 NmL-CH_4/gVS_{added} in EH2_Control following the first phase of acclimation and to 453.3 NmL-CH_4/gVS_{added} in EH3_Control after the second acclimation phase. Correspondingly, the CO_2 yield reduced from 227 NmL-CO_2/gVS_{added} to 154 NmL-CO_2/gVS_{added} and 129 NmL-CO_2/gVS_{added}, moving from EH1_Control to EH2_Control and EH3_Control respectively. So, just by a sequential acclimation, biogas was improved from 64.8% biomethane in EH1_Control to 73.9% in EH2_Control and finally 77.8% in EH3_Control.

The biogas quality was further improved by the combined effect of acclimation and a stepwise increase in H_2 in the test reactors over the respective controls. The biomethane contained in the biogas of the test reactors improved from 77.2% in EH1_Test to 78.1% in EH2_Test and 81.0% in EH3_Test, corresponding to 468.3, 483.6, and 499.0 NmL-CH_4/gVS_{added}. In comparison with the corresponding controls, the increase in percentage biomethane was 12.4%, 4.2% and 3.2% in EH1, EH2 and EH3 respectively. The observed decline in the percentage change in the biomethane yield between the control and the test is because the biomethanation was also improved in the control with sequential acclimation.

Other batch *in-situ* biomethanation studies, where more than one-time H_2 injection was made, have reported similar upgrades to the present study. Mulat et al. (2017) reported an increase in biomethane yield from 64.4% and 65.2% to 87.8% and 89.4% respectively, using two types of maize leaf as substrate. Bassani et al. (2015) also reported a biomethane increase from 69.7 to 88.9% at thermophilic temperature

and 67.1 to 85.1% at mesophilic temperature, using cattle manure as a substrate. Agneessens et al. (2017) reported improved biomethane yield ranging from 76.8 – 100% against 59.4% obtained without H_2 addition, using maize leaf as substrate. The authors further reported that yields that tended towards 100% CH_4 were due to excessive H_2 loading, which enriched homoacetogenesis, consequently, inducing VFA inhibition and accumulation.

3.3.1 Kinetic analysis

The kinetic parameters obtained from the modified Gompertz (MGompertz) fitting models (Okoro-Shekwaga et al., 2020) are summarised in **Error! Reference source not found.**. The *k*-value and maximum specific methane yield increased through the acclimation phases, consequently, reducing the lag times. The addition of H_2 to the acclimated systems (EH2_Test and EH3_Test) was observed to slightly improve the lag time and maximum specific methane yield for the corresponding acclimation phase. These changes were only small because of the resultant improvement in the control reactors. In contrast, Pan et al. (2016) reported a reduction in maximum specific methane yield and an increase in lag time by H_2 adaptation. However, they suggested it was due to a short adaptation period of one week, during which the microorganisms were assumed to be in the decay stage.

3.4 Biomethane end-use comparison

This section analyses the different options for the use of biomethane from the present study, including electricity from combined heat and power, GtG injection and vehicle fuel, as derived from different biogas upgrading technology. Bright et al. (2011) identified two important variables to compare the three end-uses: (i) The efficiency of the biogas conversion to the respective products (GtG, electricity and vehicle fuel) and (ii) The extent to which the use of the product avoids carbon emissions. Therefore, in this section, the efficiency of conversion and carbon displacements from the use of biomethane are discussed.

3.4.1 The efficiency of biogas conversion to end products

Energy yields from the present study (*in-situ* biomethanation) were compared with conventional physicochemical technologies for biogas upgrade like absorption (i.e., high-pressure water scrubbing - HPWS, and organic physical scrubbing - OPS); adsorption (i.e., amine scrubbing – AS, and pressure swing adsorption - PSA);

membrane separation (MS) and cryogenic separation (CS). Efficiencies of conversion and energy balances for H_2 addition in this study were calculated according to (i) the amount of H_2 required, (ii) energy balance based on the net energy worth from the use of biomethane and (iii) potential hydrogen sources that can easily be adapted to the process.

3.4.1.1 Amount of hydrogen gas required

The statistical relationship between percentages of H_2 utilised in the H_2-supplemented systems and methane yield was established by linear regression using the MiniTab18® statistical tool. Regression equations from nine data points obtained from the experiments (using the three gas mixtures – 5%, 10% and 15% H_2) were used for each linear regression fitting, with R^2 values in the range of 0.88 to 0.99. The resulting regression equations (Equations 4 and 5) were then used to predict the level of acclimation required to obtain higher percentages of methane in the biogas; assuming all conditions remained unchanged.

$$Biomethane\ in\ biogas\ (\%) = 74.65 + 0.40 \cdot (H_2\ added, \%) \qquad Eq.\ 4$$

$$Biomethane\ yield = 452.9 + 3.07 \cdot (H_2\ added, \%) \qquad Eq.\ 5$$

To meet higher fuel standards such as those required for GtG injection and vehicle fuel, the biomethane content needs to be above 95%; typically 97 – 98% (Bright et al., 2011). Therefore, Equation 4 was used to extrapolate the amount of H_2 required to enrich the inoculum to allow continuous production of biogas as 98% biomethane content. According to Equation 2, an equivalent of 58%-H_2 will be required to obtain 98% biomethane content by continuous acclimation. Therefore, the corresponding amount of H_2 required was calculated for a stepwise increase from 5% to 60%-H_2 (at 5% interval) – i.e. 12 acclimation steps in sequence. Based on a 21-day hydraulic retention time (HRT) as in the present study, it would require 252 days of sequential acclimation of inoculum with a stepwise increase in H_2. However, considering the VFA decomposition rates improved as acclimation progressed in the present study (see Section 3.2), the HRT could be shortened after the first few acclimation steps, to allow a shorter acclimation period

The amount of H_2 required for the sequential acclimation phase is the combined total of H_2 from each stage, i.e. – from 5% to 60% headspace volume, which is 331.5 mL equivalent to 4420 mL/L or in terms of solids, 138 mL/gVS_{added} (147 $m^3/tonne_{FW}$ on dry basis – m^3/t_{FW}) required over an acclimation period of 252 days (~17.5 mL/L(day)).

3.4.1.2 Energy balance analysis

A review of biogas upgrade, utilisation and storage was reported by Ullah Khan et al. (2017), which describes potential energy input and biomethane losses from physicochemical biogas upgrade systems. This information was used for energy balance analysis from physicochemical biogas upgrading systems in comparison with *in-situ* biomethanation – present study (**Error! Reference source not found.**). Biogas yield from the control, in which H_2 was not added was used to estimate the energy balance from conventional physicochemical technologies, assuming the obtained biogas was upgraded through such systems, taking into account the potential biomethane losses from such systems. Energy balances from these systems were then compared with the energy balance for *in-situ* biomethanation to achieve 98% biomethane as in the present study.

The biogas yield from the control was 644 NmL/gVS_{added} equivalent to 685 m^3/t_{FW}, with biomethane content of 417.6 mL-CH_4/gVS_{added} (444 m^3/t_{FW}) at 65%. The calculated biomethane yield at 98% biomethane content from *in-situ* biomethanation was 637.1 mL-CH_4/gVS_{added} (678 m^3/t_{FW}). The calorific value of biomethane from the respective upgrading processes was calculated by correcting the calorific value of pure methane (39.8 MJ/m^3) with the fractions of methane in the upgraded biogas – i.e. the methane purity (**Error! Reference source not found.**). The energy output through three end-uses (electricity, GtG and vehicle fuel) was estimated by multiplying the calorific value by the respective efficiencies: 35% for biomethane conversion to electricity by CHP (Scarlat et al., 2018), 99.75% efficiency for GtG injection (Bright et al., 2011) and 98% assumed for biomethane when used as a transport fuel.According to **Error! Reference source not found.**, upgrading the biogas increases the calorific value and energy output of the biogas and opens up additional revenue options from its end-use and using *in-situ* biomethanation over conventional physicochemical technology increases the energy return on investment

(EROI – energy output minus energy input). The energy input for physicochemical biogas upgrade is rated according to the volume of biogas to be upgraded, while the energy input for water electrolysis is rated according to the volume of H_2 required. So, although water electrolysis has a higher energy input, the volume of H_2 required to achieve 98% biomethane yield (147 m^3-H_2/t_{FW}) was smaller than the volume of biogas to be upgraded (685 m^3-biogas/t_{FW}), making the energy input within the range of some physicochemical methods. However, the energy input for *in-situ* biomethanation considered here only includes the H_2 production system and does not consider potential energy input for H_2 injection into the system. The units for H_2 injection were assumed to be similar to units used for biogas production, storage and transportation and hence, not considered in this study to have a huge impact on the energy input. The EROI if the biomethane is used for electricity is 0.2 – 1.6 MWh/t_{FW} by a physicochemical method and 1.8 MWh/t_{FW} by *in-situ* biomethanation. Upgrading biogas to meet the standards for GtG injections and vehicle fuel, the EROI increases to about 4.0 – 4.8 MWh/t_{FW} using a physicochemical method and 6.6 MWh/t_{FW} by *in*-situ biomethanation. Therefore, by *in-situ* biomethanation, about 38 – 65% increases over conventional physicochemical technologies could be achieved depending on the biomethane end-use.

3.4.1.3 Potential sources of hydrogen for in-situ biomethanation scalability

Water electrolysis stands out as a sustainable and renewable source of H_2 for biomethanation (Bekkering et al., 2020). H_2 production by water electrolysis contributes about 4% of overall annual H_2 produced around the world and was estimated to increase to about 22% in 2050 (International Energy Agency, 2006). There is, therefore, a growing interest and demand for water electrolysis, using energy from other renewable sources such as wind and solar when such systems produce energy beyond their storage capacity (Bekkering et al., 2020). For instance, over 26% of the EU's electricity from wind is temporarily surplus, which can be used for electrolysis (Ullah Khan et al., 2017). The conventional industrial electrolyser requires about 4.5 – 5 kWh energy input per m^3 of hydrogen (Rashid et al., 2015) and alkaline electrolysers are currently the most commercially available water electrolysers, having up to 150 MW capacity, which could sufficiently meet the hydrogen demand for *in-situ* biomethanation in the present study.

However, because of the current distance in separation between the respective renewable energy installations, the transportation of surplus energy from the source of production to the AD plant might yet pose some challenges. Another option for H_2 production which can be integrated into the biomethanation system is biological H_2 production by dark fermentation. Dark fermentation is likened to AD with the elimination of the methanogenesis phase, hence, it requires a similar reactor design and operation as in AD. It is considered the most promising method for the recovery of biohydrogen from biomass with a 1.9 net energy ratio (Łukajtis et al., 2018). Therefore, for current practices, dark fermentation is suggested in this study to be more easily adapted for biomethanation than water electrolysis; since its operation is similar to the conventional AD. H_2 yields in a range of 57 to 283 mL/gVS was reported from FW in a review by Uçkun Kiran et al. (2014) and the incremental H_2 required for progressive acclimation in this study was around 138 mL/gVS. Thus, dark fermentation might be able to meet short term demand for the hydrogen required for *in-situ* biomethanation, until power-to-hydrogen systems get fully developed.

3.4.2 Carbon displaced from biomethane end-use

The carbon displaced from the use of biomethane depends on the actual property of the fuel which it displaces when used (Bright et al., 2011). Energy conversion factors are used to estimate the carbon saving from the use of biomethane as different end products.

The carbon savings from the use of biomethane for GtG injection, electricity and vehicle fuel when it replaces natural gas, grid electricity and vehicle fuel (diesel and petrol) respectively, are summarised in **Error! Reference source not found.** based on energy conversion factors published by Carbon Trust (2016) and energy outputs from **Error! Reference source not found.**. Regardless of the upgrading technology, the use of biomethane as vehicle fuel would result in the highest carbon saving compared to electricity and GtG (**Error! Reference source not found.**). However, a shift from physicochemical methods to biological hydrogen methanation allows more carbon savings. Moreover, **Error! Reference source not found.** only gives a gross estimate of carbon savings, but physicochemical technologies reportedly have high parasitic CO_2 load, which often leads to a reduced net carbon saving (Bright et

al., 2011). Carbon savings estimation from the use of biomethane in 2010 revealed its use as vehicle fuel provided the best carbon saving followed by electricity (Bright et al., 2011). Lower carbon saving from GtG was due to the combined factors of (i) natural gas (which GtG replaces) being a relatively low carbon fossil fuel and (ii) the relatively high parasitic load from the physicochemical upgrade (Bright et al., 2011). The production of hydrogen from other renewable systems for use in biomethanation allows the entire process to be renewable, therefore, avoiding any parasitic carbon load arising from the upgrading process, so that the gross carbon saving from *in-situ* biomethanation on **Error! Reference source not found.** would be the same as the net carbon saving.

4. Techno-economic implications

The revenue from biogas is often dependent on prevailing government policies and incentives from the respective end-uses (Rajendran et al., 2019). Although these incentives are quite volatile, biogas upgrade for transport and GtG currently hold the best prospects for biogas in terms of the EROI and carbon saving according to the present study. According to WRAP's 2017 spreadsheet on operational AD in the UK (available online – WRAP, 2019), there are about 10 AD plants in the UK injecting biomethane to the gas grid; 2 of which are FW AD plants. Other FW AD plants primarily use biogas to operate CHP engines. From the present study, *in-situ* biomethanation can be adapted into FW AD in the UK, to increase the end-value of the biogas, which would broaden the revenue streams for AD operators and reduce the carbon arisings from FW AD. A synergistic approach among renewable energy sources would be the best option for H_2 production where possible. If that were the case, water electrolysis would give the purest and most consistent quantity of H_2 for biomethanation. However, these systems are not yet fully developed, therefore, for current practice, dark fermentation might be cheaper and more easily incorporated, since it requires similar technical know-how as in the AD system.

5. Conclusions

An acclimation to increasing concentrations of H_2 helped to improve both VFA decomposition and biogas upgrade. The accumulation of VFA (C2 – C4) declined and only valerate (C5) was observed to accumulate to higher levels in the early days

as acclimation progressed. Notwithstanding, the time taken for all monitored VFA to reach the peak and the respective concentrations at the peak greatly reduced. This connotes a faster VFA decomposition with acclimation, which would imply the avoidance of VFA-related inhibition. This was supported by an improvement in the kinetics, depicted by increases in k-value and maximum specific methane yield and a reduction in lag time. Hence, the potential VFA accumulation towards valerate instead of propionate and/or acetate reported in this study due to a stepwise increase in H_2 concentration in the acclimation phases should be further explored in future studies to reduce inhibitory effects associated with high H_2 load/partial pressure during FW AD. By acclimation to a stepwise increase in H_2 load, the biogas was upgraded to about 81% biomethane (499.0 NmL/gVS_{added}) against 65% (417.6 NmL/gVS_{added}), without H_2 addition. The progression of the *in-situ* biomethanation by H_2 acclimation to higher biogas standards that allow its use for GtG injection or as a vehicle fuel, could deliver 38 – 65% increases in EROI and 52 – 59% increases in carbon savings compared to physicochemical methods for biogas upgrade. Also, to achieve biogas upgrade by *in-situ* biomethanation, water electrolysis and dark fermentation offer sustainable options for H_2 production, with dark fermentation seemingly more easily adaptable for current practices. The interpretation made in the present study is based on experimental data, real-life tests are recommended to validate this, as part of future investigations.

Acknowledgement

The authors will like to thank the University of Leeds, the United Kingdom for the financial support of Dr Cynthia Kusin Okoro-Shekwaga through the Leeds International Research Scholarship (LIRS) and the Living Lab Sustainability Program.

References

Agneessens, L.M., Ottosen, L.D.M., Voigt, N.V., Nielsen, J.L., de Jonge, N., Fischer, C.H., Kofoed, M.V.W., 2017. In-situ biogas upgrading with pulse H2additions: The relevance of methanogen adaption and inorganic carbon level. Bioresour. Technol. 233, 256–263. https://doi.org/10.1016/j.biortech.2017.02.016

Angelidaki, I., Treu, L., Tsapekos, P., Luo, G., Campanaro, S., Wenzel, H., Kougias,

669 P.G., 2018. Biogas upgrading and utilization: Current status and perspectives.
670 Biotechnol. Adv. 36, 452–466. https://doi.org/10.1016/j.biotechadv.2018.01.011
671 APHA, 2006. Experiment on Determination of Chemical Oxygen Demand.
672 APHA, 2005. Standard Methods for the Examination of Water and Wastewater, 21st
673 ed. American Public Health Association, American Water Works Association,
674 Water Environment Federation, Washington, DC.
675 Appels, L., Baeyens, J., Degrève, J., Dewil, R., 2008. Principles and potential of the
676 anaerobic digestion of waste-activated sludge. Prog. Energy Combust. Sci. 34,
677 755–781. https://doi.org/10.1016/j.pecs.2008.06.002
678 Bassani, I., Kougias, P.G., Angelidaki, I., 2016. In-situ biogas upgrading in
679 thermophilic granular UASB reactor : key factors affecting the hydrogen mass
680 transfer rate. Bioresour. Technol. 221, 485–491.
681 https://doi.org/10.1016/j.biortech.2016.09.083
682 Bassani, I., Kougias, P.G., Treu, L., Angelidaki, I., 2015. Biogas upgrading via
683 hydrogenotrophic methanogenesis in two-stage continuous stirred tank reactors
684 at mesophilic and thermophilic conditions. Environ. Sci. Technol. 49, 12585–
685 12593. https://doi.org/10.1021/acs.est.5b03451
686 Bekkering, J., Zwart, K., Martinus, G., Langerak, J., Tideman, J., van der Meij, T.,
687 Alberts, K., van Steenis, M., Nap, J.P., 2020. Farm-scale bio-power-to-methane:
688 Comparative analyses of economic and environmental feasibility. Int. J. Energy
689 Res. 44, 2264–2277. https://doi.org/10.1002/er.5093
690 Bright, A., Bulson, H., Henderson, A., Sharpe, N., Dorstewitz, H., Pickering, J., 2011.
691 An introduction to the production of biomethane gas and injection to the national
692 grid [WWW Document]. Advant. West Midlands Waste Resour. Action Program.
693 URL http://www.wrap.org.uk/sites/files/wrap/AWM Biomethane to Grid 05 07
694 11.pdf
695 Carbon Trust, 2016. Conversion factors - energy and carbon conversion guide,
696 Carbon Trust. https://doi.org/10.1016/B978-0-444-99789-0.50006-6
697 Chen, Y., Cheng, J.J., Creamer, K.S., 2008. Inhibition of anaerobic digestion
698 process: A review. Bioresour. Technol. 99, 4044–4064.
699 https://doi.org/10.1016/j.biortech.2007.01.057
700 Defra, 2011. Anaerobic Digestion Strategy and Action Plan: A commitment to

701 increasing energy from waste through Anerobic Digestion [WWW Document].
702 Dep. Environ. Food Rural Aff. URL
703 https://assets.publishing.service.gov.uk/government/uploads/system/uploads/a
704 ttachment_data/file/69400/anaerobic-digestion-strat-action-plan.pdf
705 Demirel, B., Scherer, P., 2008. The roles of acetotrophic and hydrogenotrophic
706 methanogens during anaerobic conversion of biomass to methane: A review.
707 Rev. Environ. Sci. Biotechnol. 7, 173–190. https://doi.org/10.1007/s11157-008-
708 9131-1
709 Evangelisti, S., Lettieri, P., Borello, D., Clift, R., 2014. Life cycle assessment of
710 energy from waste via anaerobic digestion: A UK case study. Waste Manag. 34,
711 226–237. https://doi.org/10.1016/j.wasman.2013.09.013
712 Fukuzaki, S., Nishio, N., Shobayashi, M., Nagai, S., 1990. Inhibition of the
713 fermentation of propionate to methane by hydrogen, acetate, and propionate.
714 Appl. Environ. Microbiol. 56, 719–723.
715 Gallert, C., Winter, J., 2008. Propionic acid accumulation and degradation during
716 restart of a full-scale anaerobic biowaste digester. Bioresour. Technol. 99, 170–
717 178. https://doi.org/10.1016/j.biortech.2006.11.014
718 Gao, S., Zhao, M., Chen, Y., Yu, M., Ruan, W., 2015. Tolerance response to in situ
719 ammonia stress in a pilot-scale anaerobic digestion reactor for alleviating
720 ammonia inhibition. Bioresour. Technol. 198, 372–379.
721 https://doi.org/10.1016/j.biortech.2015.09.044
722 Girotto, F., Alibardi, L., Cossu, R., 2015. Food waste generation and industrial uses:
723 A review. Waste Manag. 45, 32–41.
724 https://doi.org/10.1016/j.wasman.2015.06.008
725 Gu, J., Liu, R., Cheng, Y., Stanisavljevic, N., Li, L., Djatkov, D., Peng, X., Wang, X.,
726 2020. Anaerobic co-digestion of food waste and sewage sludge under
727 mesophilic and thermophilic conditions: Focusing on synergistic effects on
728 methane production. Bioresour. Technol. 301, 122765.
729 https://doi.org/10.1016/j.biortech.2020.122765
730 Holliger, C., Alves, M., Andrade, D., Angelidaki, I., Astals, S., Baier, U., Bougrier, C.,
731 Buffière, P., Carballa, M., De Wilde, V., Ebertseder, F., Fernández, B., Ficara,
732 E., Fotidis, I., Frigon, J.C., De Laclos, H.F., Ghasimi, D.S.M., Hack, G., Hartel,

M., Heerenklage, J., Horvath, I.S., Jenicek, P., Koch, K., Krautwald, J., Lizasoain, J., Liu, J., Mosberger, L., Nistor, M., Oechsner, H., Oliveira, J.V., Paterson, M., Pauss, A., Pommier, S., Porqueddu, I., Raposo, F., Ribeiro, T., Pfund, F.R., Strömberg, S., Torrijos, M., Van Eekert, M., Van Lier, J., Wedwitschka, H., Wierinck, I., 2016. Towards a standardization of biomethane potential tests. Water Sci. Technol. 74, 2515–2522. https://doi.org/10.2166/wst.2016.336

International Energy Agency, 2006. Technology roadmap: hydrogen and fuel cells, in: Encyclopedia of Production and Manufacturing Management. pp. 781–782. https://doi.org/10.1007/1-4020-0612-8_961

Lee, C., Kim, J., Hwang, K., O'Flaherty, V., Hwang, S., 2009. Quantitative analysis of methanogenic community dynamics in three anaerobic batch digesters treating different wastewaters. Water Res. 43, 157–165. https://doi.org/10.1016/j.watres.2008.09.032

Lim, L.Y., Klemeš, J.J., Ho, C.S., Ho, W.S., Lee, C.T., Bong, C.P.C., 2017. The characterisation and treatment of food waste for improvement of biogas production during anaerobic digestion – A review. J. Clean. Prod. 172, 1545–1558. https://doi.org/10.1016/j.jclepro.2017.10.199

Liu, T., Sung, S., 2002. Ammonia inhibition on thermophilic aceticlastic methanogens. Water Sci. Technol. 45, 113–120.

Łukajtis, R., Hołowacz, I., Kucharska, K., Glinka, M., Rybarczyk, P., Przyjazny, A., Kamiński, M., 2018. Hydrogen production from biomass using dark fermentation. Renew. Sustain. Energy Rev. 91, 665–694. https://doi.org/10.1016/j.rser.2018.04.043

Luo, G., Angelidaki, I., 2013. Co-digestion of manure and whey for in situ biogas upgrading by the addition of H2: Process performance and microbial insights. Appl. Microbiol. Biotechnol. 97, 1373–1381. https://doi.org/10.1007/s00253-012-4547-5

Mirmohamadsadeghi, S., Karimi, K., Tabatabaei, M., Aghbashlo, M., 2019. Biogas production from food wastes: A review on recent developments and future perspectives. Bioresour. Technol. Reports 7, 100202. https://doi.org/10.1016/j.biteb.2019.100202

765 Mulat, D.G., Mosbæk, F., Ward, A.J., Polag, D., Greule, M., Keppler, F., Nielsen,
766 J.L., Feilberg, A., 2017. Exogenous addition of H2 for an in situ biogas
767 upgrading through biological reduction of carbon dioxide into methane. Waste
768 Manag. 68, 146–156. https://doi.org/10.1016/j.wasman.2017.05.054
769 Muñoz, R., Meier, L., Diaz, I., Jeison, D., 2015. A review on the state-of-the-art of
770 physical/chemical and biological technologies for biogas upgrading. Rev.
771 Environ. Sci. Biotechnol. 14, 727–759. https://doi.org/10.1007/s11157-015-
772 9379-1
773 Okoro-Shekwaga, C.K., Ross, A.B., Camargo-Valero, M.A., 2019. Improving the
774 biomethane yield from food waste by boosting hydrogenotrophic
775 methanogenesis. Appl. Energy 254, 113629.
776 https://doi.org/10.1016/j.apenergy.2019.113629
777 Okoro-Shekwaga, C.K., Turnell Suruagy, M.V., Ross, A., Camargo-Valero, M.A.,
778 2020. Particle size, inoculum-to-substrate ratio and nutrient media effects on
779 biomethane yield from food waste. Renew. Energy 151, 311–321.
780 https://doi.org/10.1016/j.renene.2019.11.028
781 Pan, X., Angelidaki, I., Alvarado-Morales, M., Liu, H., Liu, Y., Huang, X., Zhu, G.,
782 2016. Methane production from formate, acetate and H2/CO2; focusing on
783 kinetics and microbial characterization. Bioresour. Technol. 218, 796–806.
784 https://doi.org/10.1016/j.biortech.2016.07.032
785 Rajagopal, R., Massé, D.I., Singh, G., 2013. A critical review on inhibition of
786 anaerobic digestion process by excess ammonia. Bioresour. Technol. 143,
787 632–641. https://doi.org/10.1016/j.biortech.2013.06.030
788 Rajendran, K., O'Gallachoir, B., Murphy, J.D., 2019. The combined role of policy and
789 incentives in promoting cost efficient decarbonisation of energy: A case study
790 for biomethane. J. Clean. Prod. 219, 278–290.
791 https://doi.org/10.1016/j.jclepro.2019.01.298
792 Rashid, M., Khaloofah, M., Mesfer, A., Naseem, H., Danish, M., Al Mesfer, M.K.,
793 2015. Hydrogen production by water electrolysis: A review of alkaline water
794 electrolysis, PEM water electrolysis and high temperature water electrolysis. Int.
795 J. Eng. Adv. Technol. 2249–8958.
796 Savvas, S., Donnelly, J., Patterson, T., Chong, Z.S., Esteves, S.R., 2017. Biological

797 methanation of CO2in a novel biofilm plug-flow reactor: A high rate and low
798 parasitic energy process. Appl. Energy 202, 238–247.
799 https://doi.org/10.1016/j.apenergy.2017.05.134
800 Scarlat, N., Dallemand, J.F., Fahl, F., 2018. Biogas: Developments and perspectives
801 in Europe. Renew. Energy 129, 457–472.
802 https://doi.org/10.1016/j.renene.2018.03.006
803 Shi, X., Lin, J., Zuo, J., Li, P., Li, X., Guo, X., 2017. Effects of free ammonia on
804 volatile fatty acid accumulation and process performance in the anaerobic
805 digestion of two typical bio-wastes. J. Environ. Sci. (China) 55, 49–57.
806 https://doi.org/10.1016/j.jes.2016.07.006
807 Tao, B., Alessi, A.M., Zhang, Y., Chong, J.P.J., Heaven, S., Banks, C.J., 2019.
808 Simultaneous biomethanisation of endogenous and imported CO2 in organically
809 loaded anaerobic digesters. Appl. Energy 247, 670–681.
810 https://doi.org/10.1016/j.apenergy.2019.04.058
811 Tao, B., Zhang, Y., Heaven, S., Banks, C.J., 2020. Predicting pH rise as a control
812 measure for integration of CO2 biomethanisation with anaerobic digestion. Appl.
813 Energy 277, 115535. https://doi.org/10.1016/j.apenergy.2020.115535
814 Tian, H., Fotidis, I.A., Mancini, E., Treu, L., Mahdy, A., Ballesteros, M., González-
815 Fernández, C., Angelidaki, I., 2018. Acclimation to extremely high ammonia
816 levels in continuous biomethanation process and the associated microbial
817 community dynamics. Bioresour. Technol. 247, 616–623.
818 https://doi.org/10.1016/j.biortech.2017.09.148
819 Treu, L., Kougias, P.G.G., de Diego-Díaz, B., Campanaro, S., Bassani, I.,
820 Fernández-Rodríguez, J., Angelidaki, I., 2018. Two-year microbial adaptation
821 during hydrogen-mediated biogas upgrading process in a serial reactor
822 configuration. Bioresour. Technol. 264, 140–147.
823 https://doi.org/10.1016/j.biortech.2018.05.070
824 Uçkun Kiran, E., Trzcinski, A.P., Ng, W.J., Liu, Y., 2014. Bioconversion of food waste
825 to energy: A review. Fuel 134, 389–399.
826 https://doi.org/10.1016/j.fuel.2014.05.074
827 Ullah Khan, I., Hafiz Dzarfan Othman, M., Hashim, H., Matsuura, T., Ismail, A.F.,
828 Rezaei-DashtArzhandi, M., Wan Azelee, I., 2017. Biogas as a renewable energy

fuel – A review of biogas upgrading, utilisation and storage. Energy Convers. Manag. 150, 277–294. https://doi.org/10.1016/j.enconman.2017.08.035

Wahid, R., Mulat, D.G., Gaby, J.C., Horn, S.J., 2019. Effects of H2:CO2 ratio and H2 supply fluctuation on methane content and microbial community composition during in-situ biological biogas upgrading. Biotechnol. Biofuels 12. https://doi.org/10.1186/s13068-019-1443-6

Wang, L., Zhou, Q., Li, F.T., 2006. Avoiding propionic acid accumulation in the anaerobic process for biohydrogen production. Biomass and Bioenergy 30, 177–182. https://doi.org/10.1016/j.biombioe.2005.11.010

Wang, L.H., Wang, Q., Cai, W., Sun, X., 2012. Influence of mixing proportion on the solid-state anaerobic co-digestion of distiller's grains and food waste. Biosyst. Eng. 112, 130–137. https://doi.org/10.1016/j.biosystemseng.2012.03.006

Wang, Q., Kuninobu, M., Ogawa, H.I., Kato, Y., 1999. Degradation of volatile fatty acids in highly efficient anaerobic digestion. Biomass and Bioenergy 16, 407–416. https://doi.org/10.1016/S0961-9534(99)00016-1

WRAP, 2019. Operational AD sites | WRAP UK [WWW Document]. URL http://www.wrap.org.uk/content/operational-ad-sites (accessed 2.15.19).

WRAP, 2017. Estimates of food surplus and waste arisings in the UK, Wrap.

Yang, Y., Chen, Q., Guo, J., Hu, Z., 2015. Kinetics and methane gas yields of selected C1 to C5 organic acids in anaerobic digestion. Water Res. 87, 112–118. https://doi.org/10.1016/j.watres.2015.09.012

Yang, Y., Zhang, Y., Li, Z., Zhao, Zhiqiang, Quan, X., Zhao, Zisheng, 2017. Adding granular activated carbon into anaerobic sludge digestion to promote methane production and sludge decomposition. J. Clean. Prod. 149, 1101–1108. https://doi.org/10.1016/j.jclepro.2017.02.156

Yenigün, O., Demirel, B., 2013. Ammonia inhibition in anaerobic digestion : A review. Process Biochem. 48, 901–911. https://doi.org/10.1016/j.procbio.2013.04.012

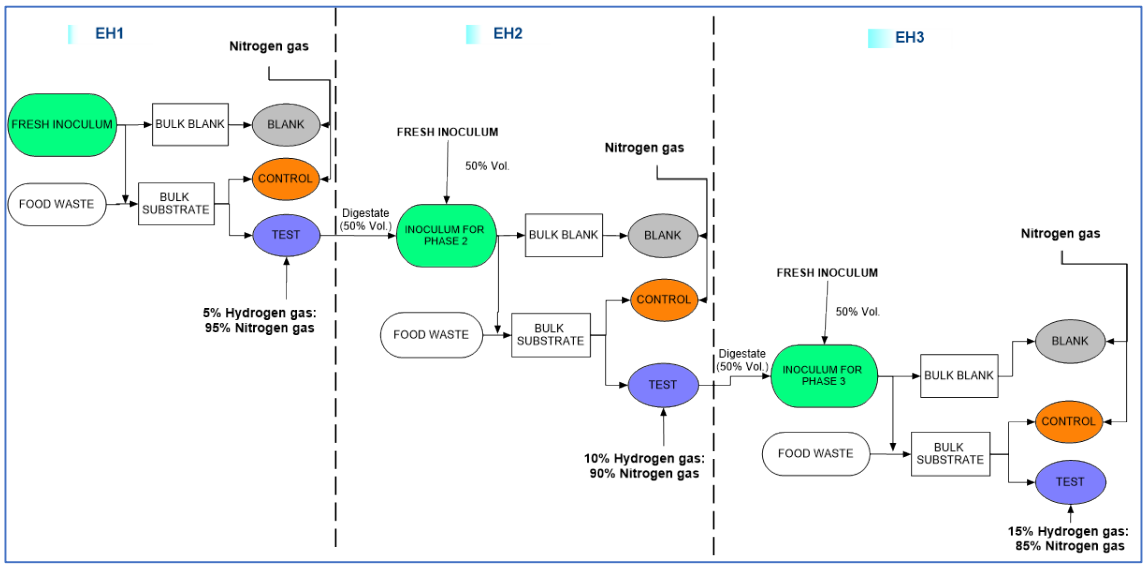

857

858 *Figure 1. Experimental design for enhanced biomethanation from food waste*
859 *via sequential inoculum acclimation by H_2 addition*

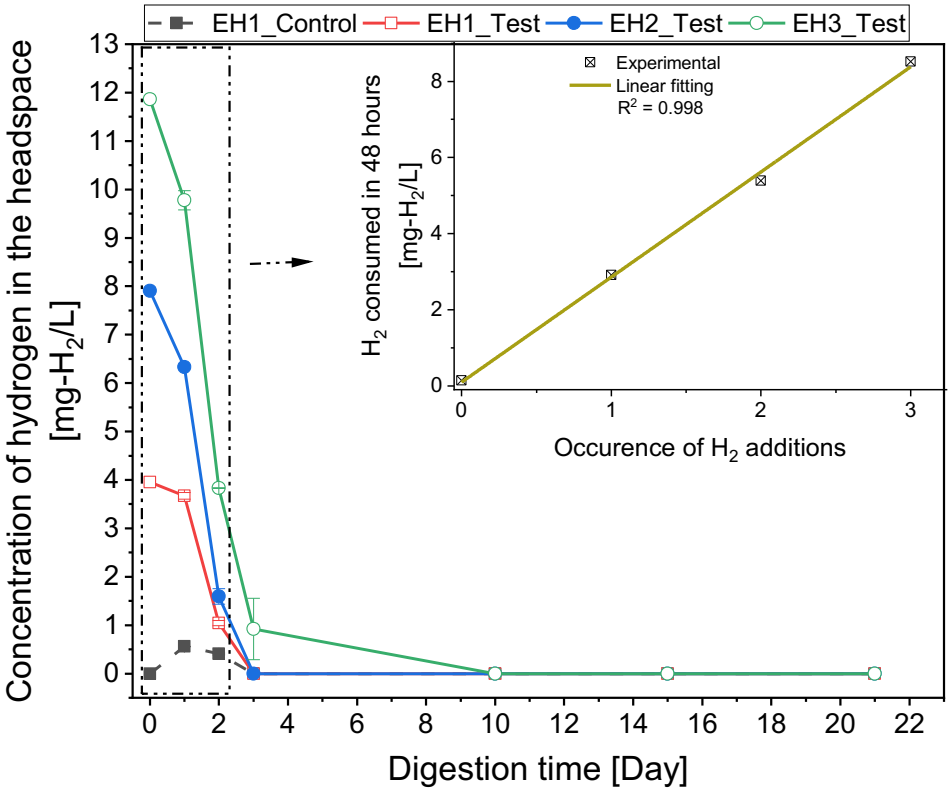

Figure 2. Changes in headspace H_2 concentration as an indication of H_2 gas-liquid transfer (H_2 was not detected in EH2_Control and EH3_Control).

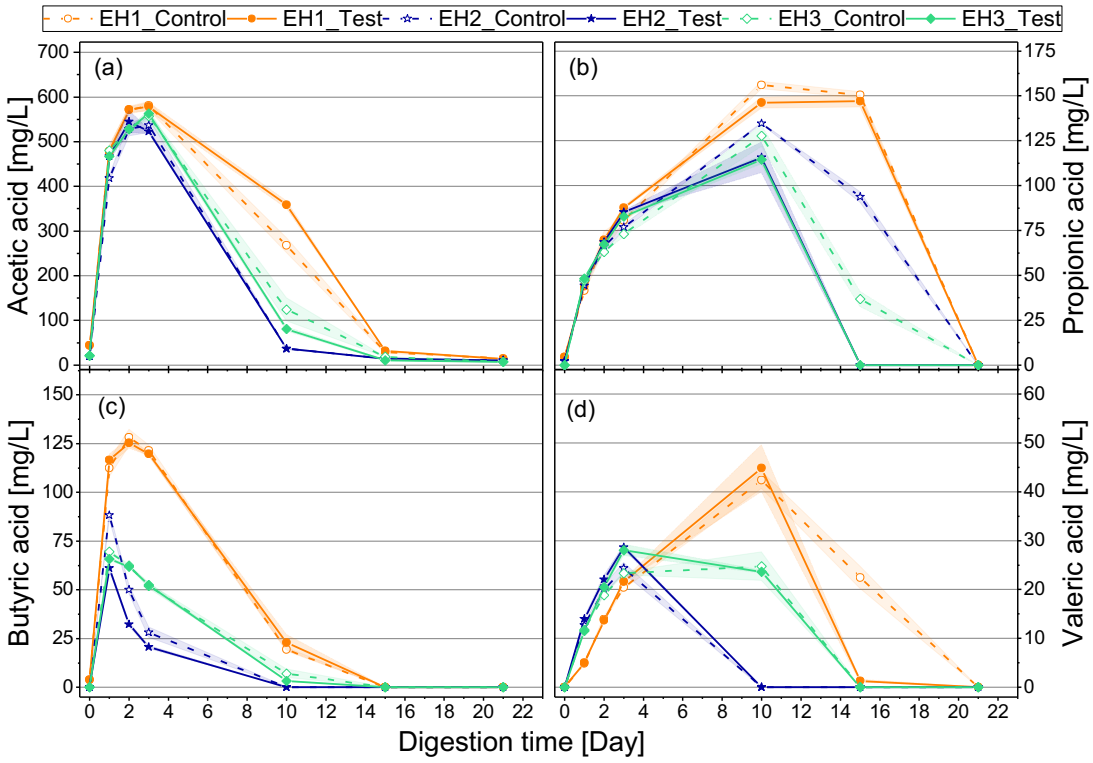

Figure 3. Effects of hydrogen acclimation on VFA composition: test values presented in solid lines and control in dash lines. The shaded area around the lines represents the standard deviation from the mean.

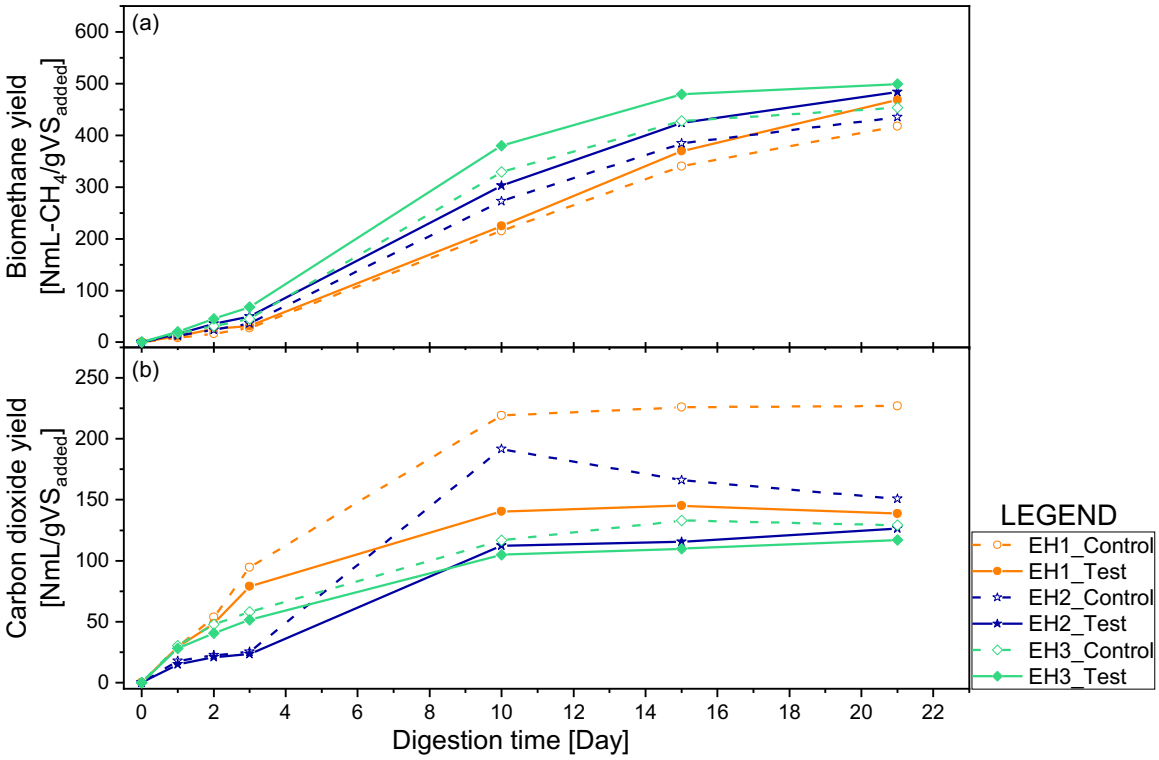

870

871 *Figure 4. Biomethane (a) and Carbon dioxide (b) production curves from all*
872 *hydrogen-based acclimation experiments: dash lines represent*
873 *control yields and the solid lines represent test yields.*

874 *Table 1. Characteristics of FW and initial reactor liquid content**

Parameter	FW	EH1 (control and test)	EH2 (control and test)	EH3 (control and test)
pH	4.80	8.49	8.52	8.54
VS (g/L)	295.0 (0.3)[a]	9.0 (0.2)	10.4 (0.3)	8.0 (0.1)
TS (g/kL)	314.3 (0.2)[a]	14.3 (0.2)	16.7 (0.5)	12.8 (0.3)
TCOD (g/L)	469.7 (0.0)[a]	26.1 (0.5)	11.6 (0.0)	13.3 (0.3)
sCOD (g/L)	--	2.0 (0.1)	2.0 (0.0)	1.7 (0.0)
VFA (mg/L)	5111 (354)[a]	52.1 (1.5)	15.8 (6.3)	21.2 (0.1)
C (% of TS)	53.19 (2.12)	31.26 (0.41)	31.05 (0.30)	32.31 (0.31)
H (% of TS)	7.87 (0.23)	4.60 (0.01)	4.05 (0.05)	3.42 (0.14)
N (% of TS)	4.44 (0.10)	4.02 (0.03)	4.09 (0.03)	4.53 (0.12)
S (% of TS)	0.33(0.18)	1.08 (0.05)	0.94 (0.02)	0.45 (0.06)
C/N	12.0	7.8	7.6	7.1
TMP (mL/gVS)	588.63	--	--	--

875 VS – volatile solids; TS – total solids; TCOD – total chemical oxygen demand; sCOD – soluble chemical oxygen demand; C –
876 carbon; N – nitrogen; H – hydrogen; S – sulphur and TMP – Theoretical methane potential
877 [a]VS, TS and TCOD presented in g/kg and VFA in mg/kg
878 *Mean values from replicates are reported with standard deviations in bracket (n = 3)
879

880 *Table 2. Kinetic analysis of biomethane production.*

Condition	**Experiment**	***k*-value**	**Lag time (Day)**	**Maximum specific CH_4 yield (NmL/gVS·day)**	R^2
Acclimation only	EH1_Control	0.19	3.2	31.5	0.99
	EH2_Control	0.22	2.5	37.3	0.99
	EH3_Control	0.27	2.2	45.5	0.99
Acclimation + hydrogen	EH1_Test	0.17	3.1	32.9	0.99
	EH2_Test	0.21	2.2	39.6	0.99
	EH3_Test	0.27	1.8	51.2	0.99

881

Table 3. Comparative energy outputs and caloric values from conventional upgrading technologies and this study[a].

Upgrading technology	Energy input ($kWh/m^3_{bio\ gas}$)	Energy input (MWh/t_{FW})	Methane loss (%)	Final yield (m^3CH_4/t_{FW})	Methane purity (%)	Calorific value (MJ/t_{FW})	Energy output from End use[b] (MWh/t_{FW})		
							CHP	GtG	Transport
Absorption (high-pressure water scrubbing – HPWS)	0.20 –0.43*	0.44 – 0.94	5.13*	421.5	98	16439	0.5	4.6	4.6
Absorption (chemical scrubbing – AS)	0.12 – 0.65	0.26 – 1.42	0.1*	443.8	99	17487	1.7	4.8	4.8
Absorption (organic physical scrubbing – OPS)	0.40 –0.51*	0.87 – 1.11	4*	426.5	97	16465	1.6	4.6	4.6
Adsorption (pressure swing adsorption – PSA)	0.24 –0.60*	0.52 – 1.31	4*	426.5	97.5	16550	1.6	4.6	4.6
Membrane separation – MS	0.19–0.77*	0.41 – 1.68	6*	417.6	91 – 99**	16454	1.6	4.6	4.6
Cryogenic separation – CS	0.42*	0.92	0.65*	441.4	98	17215	1.7	4.8	4.8
In-situ Biomethanation (present study)	4.5 – 5.0[c]	~0.7	-	677.8	98	26436	2.6	7.3	7.3

[a] t_{FW} = tonnes of food waste on a dry basis
[b] 1 MWh = 3600 MJ
[c] Energy input for water electrolysis at kWh per m^3 of hydrogen produced (Rashid et al., 2015). Energy input estimated for 147 m^3/t_{FW} of H_2 required in this study.
*Data obtained from Ullah Khan et al. (2017)
**91% reported by Ullah Khan et al. (2017), and 97 – 99% was reported by Muñoz et al. (2015), therefore, the maximum of 99% was adopted.

Table 4. Comparative carbon saving of biomethane per tonne of FW (dry basis) from different upgrading processes as it replaces different fuel options

Fuel	**Conversion factor***	**HPWS**	**AS**	**OPS**	**PSA**	**MS**	**CS**	**Present study (*in-situ* biomethantion)**
Unit	$kgCO_2e/kWh$	$kgCO_2e$	$kgCO_2e$	$kgCO_2e$	$kgCO_2e$	$kgCO_2e$	$kgCO_2e$	$kgCO_2e$
Grid electricity	0.412	206	700.4	659.2	659.2	659.2	700.4	1071.2
Natural gas	0.184	846.4	883.2	846.4	846.4	846.4	883.2	1343.2
Vehicle fuel	0.240	1104	1152	1104	1104	1104	1152	1752

*Source: (Carbon Trust, 2016). The conversion factor for vehicle fuel presented here as an average for diesel (0.24592 kg CO2e/kWh) and petrol (0.23324 kg CO2e/kWh).